Available online at www.sciencedirect.com
SCIENCE DIRECT®
Journal of Solid State Chemistry 177 (2004) 4213–4220
JOURNAL OF SOLID STATE CHEMISTRY
www.elsevier.com/locate/jssc

Preparation and optical spectroscopy of Eu^{3+}-doped GaN luminescent semiconductor from freeze-dried precursors

Abdelouahad El-Himri[a], Domingo Pérez-Coll[a], Pedro Núñez[a,*], Inocencio R. Martín[b], Victor Lavín[b], Vicente D. Rodríguez[b]

[a] *Departamento de Química Inorgánica, Universidad de La Laguna, c\ Avenida Astrofisico Francisco, E-38200 La Laguna, Santa Cruz de Tenerife, Spain*
[b] *Departamento de Física Fundamental y Experimental, Electrónica y Sistemas, Universidad de La Laguna, E-38200 La Laguna, Tenerife, Spain*

Received 7 May 2004; received in revised form 23 July 2004; accepted 3 August 2004

Abstracts

Pure and 0.5% and 5 mol% Eu^{3+} doped GaN nanoparticles have been prepared by ammonolysis of the corresponding freeze-dried precursors. A single hexagonal phase with the wurtzite structure was obtained as determined by X-ray Powder Diffraction. The crystallite size determined by XRD was lower than 10 nm. From optical spectroscopy characterization, it is found that the Eu_2O_3 formation is avoided by using nitrates as starting reagent. Fluorescence line narrowing spectra show excitation wavelength dependence, which is indicative that the Eu^{3+} ions are well dispersed in the prepared samples. The environment distribution occupied by the Eu^{3+} ions has been analyzed by crystal-field calculation and the results are compared with those for other materials.

Keywords: Europium doped; Gallium nitride; Freeze-dried precursor; Luminescence

1. Introduction

Group 13 nitride semiconductors have potential applications in optoelectronic devices, such as light-emitting diodes, high-intensity blue lasers and full color displays [1–3]. These materials show wide band gaps in the ultraviolet (UV) and visible (VIS) range, i.e. E_g (eV) = 6.2 (AlN), 3.4 (GaN) and 1.9 (InN). The ternary mixed phases of these nitrides are tunable emitters from red (1.9 eV) to UV (6.2 eV) depending on the stoichiometric Al:Ga or Ga:In ratio. Additionally, when these semiconductors are doped with rare earth ions show also potential applications in electroluminescent devices [4]. The doped wide-gap semiconductors, as GaN, are especially interesting because of the increasing of the rare earth ion luminescence efficiency as compared with other semiconductors such as Si or GaAs [5]. When the materials are obtained as nanopowder the quantum confinement produces important changes in their optical properties (see, for example, Ref. [6]).

Several forms of GaN can be prepared. It is possible to obtain GaN as a thin film by applying a deposition process, being the metal–organic chemical vapor deposition (MOCVD) the most important method [7–12]. These thin films of pure GaN are most often synthesized by dual source chemical vapor deposition (CVD) processes [13,14]. However, it has been shown that molecular single source precursors are both chemically and structurally attractive alternatives for the low-temperature synthesis of GaN films, powders and nanostructured solids. Inorganic and organometallic single source gallium precursors with nitrogen ligands consisting of azides [15–21], amides [22–28], hydrazines [17,29] and hydrides [30] have been utilized for GaN film and powder synthesis, being the reaction temperature of these processes in the range of 873–1273 K. Polycrystalline powders of GaN have been also prepared using gallium oxides, halides and nitrates [31,32], some of them prepared by Aerosol Assisted Vapor Phase

*Corresponding author. Fax: +34-922-318461.
E-mail address: pnunez@ull.es (P. Núñez).

0022-4596/$ - see front matter © 2004 Elsevier Inc. All rights reserved.
doi:10.1016/j.jssc.2004.08.004

Synthesis (AAVS). The solid solution $In_xGa_{1-x}N$ ($x = 0$, 0.5, 1.0) has been prepared by pyrolysis of ammoniumhexafluoroindategallate in ammonia flow [33].

Rare earth doped GaN has been generally obtained as films by means of metalorganic molecular beam epitaxy (MOMBE) or by ion implantation [34]. This is because most of the precursor methods mentioned above have not been applied to systems where dopant control is required. We must comment a work concerning to the preparation of GaN:Eu via chemistry by ammonolysis, as this article, but using ammoniumhexafluorometallate as precursor [35]. The special properties of the trivalent lanthanide ions are due to the incomplete inner 4f shell that gives rise to paramagnetic properties and the interaction with UV, VIS or IR radiation. The coordination number and the local symmetry of the ligands around the lanthanide ion rule these properties. However, the influence of the ligands is not as strong as for the transition metals, since the 4*f* orbitals in lanthanide ions are shielded from outside fields of the ligands, known as the crystal-field interaction, by the filled 5*s* and 5*p* outer shells.

Materials doped with lanthanide ions have been intensively studied in the last decades to obtain precise information on the possible environment of the lanthanide ion and its distribution in condensed matter. For this kind of study the best choice, and the most extended one, is doping with the Eu^{3+} ion. This is because it has a relatively simple energy level diagram, its optical transitions are very sensitive to the environment and the ground level $^7F_0$ and the lowest emitting level $^5D_0$ are non-degenerate; which allows applying Fluorescence Line Narrowing (FLN) techniques. So, GaN films doped with Eu^{3+}, obtained by MOMBE, have been studied by different authors [36,37].

In this paper we propose an alternative synthesis method to those expensive ones (i.e. MOMBE) for the preparation of GaN doped with Eu^{3+} as a nanostructured material by the ammonolysis of the corresponding freeze-dried precursors. Pure and Eu^{3+}-doped GaN have been prepared by this method and they have been characterized by X-ray powder diffraction, Scanning Electron Microscope (SEM) and Optical Spectroscopy.

2. Experimental

2.1. Preparation procedure

Materials used as reagents in the current investigation were: $Ga(NO_3)_3 \cdot 6H_2O$ (Aldrich 99.9%), $Eu(NO_3) \cdot 5H_2O$ (Aldrich 99.9%), $GaCl_3$ (Aldrich 99.9%), $EuCl_3$ (Aldrich 99.9%), GaF_3 (from Ga_2O_3 (Aldrich 99.99%) + HF (Merck 48%)) and EuF_3 (Aldrich 99.9%). Aqueous solutions of different compositions Ga:Eu were prepared in the adequate proportion (Ga was doped with Eu^{3+} in 0%, 0.5% or 5%) with a total cationic concentration of 0.5 M.

Droplets of these solutions (50 mL) were flash frozen by projection into liquid nitrogen and then freeze-dried at a pressure of 1–10 Pa in a Heto Lyolab 3000 freeze-drier. In this way, dried solid precursors were obtained as amorphous (X-ray diffraction) powders.

GaN, pure and doped with Eu^{3+}, were synthesized by ammonolysis of their corresponding precursors. The gases employed in the ammonolysis process were NH_3 (99.9%) and N_2 (99.9995%). A sample of the selected precursor was placed into an alumina boat and then inserted into a quartz flow-through tube furnace. The gas output of the tube furnace was connected to an acetic acid trap and the input was connected to the gas line. Prior to initiating the thermal treatment, the tube furnace was purged for 15 min with N_2 and another 15 min with NH_3. Several runs under different experimental conditions were also performed in order to determine the appropriate conditions for the preparation of pure samples. The precursor powder was heated at $5\,K\,min^{-1}$ to different final temperatures (1023–1273 K) that was held for a period of time under flowing ammonia ($50\,cm^3\,min^{-1}$). Then, the solid was cooled down at different variable rates in the same atmosphere in order to evaluate the influence of the cooling rate. The different cooling rates were obtained by either turning off the oven or leaving the sample inside (slow cooling, ca. $4\,K\,min^{-1}$) or by quenching at room temperature (fast cooling, ca. $50\,K\,min^{-1}$). The resulting materials were manipulated and stored in a dry box (Mbraum, $[O_2] < 1$ ppm; $[H_2O] < 1$ ppm).

2.2. Characterization

2.2.1. Elemental analysis

Gallium and europium contents were determined in the final nitrides (gallium doped with Eu^{3+} (at. %) 0.5% and 5%) by energy dispersive analysis of X-ray (EDAX) on a Jeol JSM 6300 SEM that was collected by an Oxford detector with quantification performed using virtual standards on associated Link-Isis software. The operating voltage was 20 kV. The nitrogen content of the nitrides was evaluated by standard combustion analysis (EA 1108 CHNS-O); N_2 and CO were separated in a chromatographic column and measured using a thermal conductivity detector.

2.2.2. X-ray diffraction

X-ray powder diffraction patterns were obtained from a Phillips X'pert automated diffractometer using graphite-monochromated Cu$K\alpha$ radiation. The diffraction patterns were performed using a special sample holder for air-sensitive samples with a Mylar cover. This sample holder was filled in a dry box. Routine patterns

for phase identification were collected with a scanning step of 0.02° (2θ), over the angular range of 10–120° (2θ), with a collection time of 5 s per step. All graphical representations relating to X-ray powder diffraction patterns were performed using the WinPLOTR program [38].

2.2.3. Microstructural characterization

The morphology of the resulting nitrides was observed using a SEM (Hitachi S-4100) operating at an accelerating voltage of 30 kV. All the preparations were covered with a thin film of gold for better image definition.

2.2.4. Optical measurements

A 6 mm-diameter pellet of the doped material was prepared using a manual press inside the dry box. Broadband emission spectra were obtained by exciting the samples with the light from a 250 W incandescent lamp passed through a 0.25 m single-grating monochromator. Fluorescence was detected through a 0.25 m double-grating monochromator with a photomultiplier. The spectra were corrected by the instrumental response. For the FLN measurements a tunable pulsed dye laser was used as an excitation source. The pulse duration was 5 ns and the repetition rate was 20 Hz. The energy density in pulsed excitation was under 0.2 mJ on 2 mm^2. The dye laser was pumped by the 532 nm pulsed light from a doubled Nd-YAG laser. For low temperature measurements a helium continuous flow cryostat was used in the range 13–300 K.

3. Results and discussion

The freeze-drying method provides a potentially simple, economic method for preparing materials with excellent control over purity, particle morphology and dopant ratio. The control of the dopant ratio is a very important factor when preparing doped materials. Most of the metalorganic phases proposed for GaN can not be used in the preparation of lanthanide doped GaN i.e. GaN:x%Ln, if the lanthanide percentage (x%) should be varied. This is because the gallium and the metal-dopant (i.e. lanthanide metal) with a given ligand do not usually fit in the same coordination number and geometry, neither in the metal/ligand ratio. In the freeze-dried precursor method the solution containing the metal salts is flash-freezed by dropping into nitrogen liquid, having homogeneity at near atomic level. Consequently, doped GaN can be prepared with any Ga dopant ratio by freeze-dried precursor method. In this work we have applied this method to prepare precursors of pure and Eu^{3+} doped GaN, which were later decomposed by ammonolysis at high temperature. Starting materials have an important effect on the crystalline level of the final materials. When gallium fluorides and chlorides were used as starting materials, the Bragg peaks of the final product were very broad and rather small. On the contrary, when gallium nitrates were used the crystalline degree was good enough from XRD data. Moreover, in the samples prepared from fluorides or chlorides peaks corresponding to Eu_2O_3 appear in the optical spectra, as will be shown later. Eu_2O_3 cannot be detected by XRD due to its low concentration in the GaN matrix. As a conclusion, the fluoride and chloride salts are not suitable as starting reagents.

GaN has two common crystal structures, the thermodynamically stable wurtzite structure and the metastable zinc blende structure [39]. The wurtzite structure has a hexagonal unit cell in the space group $P6_3mc$ and thus two lattice constants $a = 3.1892(9)$ Å and $c = 5.1850(5)$ Å. However, the zinc blende structure has a cubic unit cell with space group $F4_3m$ and the lattice parameter varies between 4.49 and 4.55 Å.

Single phase of GaN (hexagonal system of space group $P6_3mc$) has been prepared by the ammonolysis of a freeze-dried precursor heating over 873 K during 2 h and with slow or fast cooling, using gallium nitrate as starting material. But the material used in this work, with a high crystallinity degree, has been obtained at 1273 K (Fig. 1).

0.5% and 5% of Eu^{3+} doped GaN have been prepared using as starting materials metallic nitrates and by ammonolysis of the corresponding freeze-dried precursors with the same synthesis conditions that for the pure GaN. From the X-ray diffraction patterns, we confirmed that a single hexagonal phase (GaN, JCPDS Card #88-948) was obtained for both pure and Eu^{3+} doped GaN (Fig. 1).

The particle morphology was observed by Scanning Electronic Microscope for GaN samples. The nanometer particles of GaN are loosely agglomerated

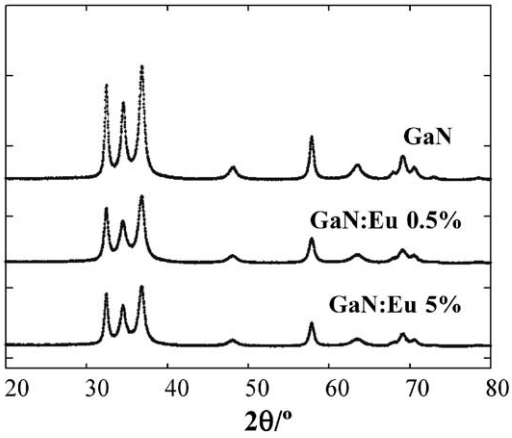

Fig. 1. X-ray diffraction pattern of GaN, GaN:Eu 0.5% and GaN:Eu 5%, obtained from nitrates.

(60–250 nm). The majority of particles inside the agglomerate are smaller than 50 nm (Figs. 2a and b). GaNs doped with Eu^{3+} have shown a similar morphology (Figs. 2c and d).

The crystallite size has been determined from XRD pattern by a standard Scherrer analysis of the half-width of the Bragg peaks, following the method described elsewhere [40]. LaB6 from NIST (SRM660a) was used as standard to calibrate the intrinsic width associated to the equipment. The sizes of the crystallites were 9 nm (GaN), 7 nm (GaN:Eu 0.5%) and 8 nm (GaN:Eu 5%)

Emission and excitation spectra of the Eu^{3+} ions in these nanomaterials were obtained from 13 K to room temperature. After excitation to the $^5D_0$ level, different visible emissions were observed that could be assigned to the $^5D_0 \rightarrow {}^7F_J$ ($J=0$–4) Eu^{3+} ion transitions.

The excitation spectra of the $^5D_0$ level of the Eu^{3+} ions, obtained for the different prepared materials, show a broad peak at 578.5 nm that would be associated to GaN:Eu, see Fig. 3. The broadening of this peak indicates the presence of a site distribution for the Eu^{3+} ions. Additional narrow peaks are also observed in the samples prepared from fluorides and from chlorides, the two most intense peaks at about 580 nm are in good agreement with those observed by Sheng and Korenowski in monoclinic Eu_2O_3 crystals [41]; this assignment will be confirmed afterwards by the emission spectra. It would be remarked that in the samples obtained from nitrates and manipulated in a dry box the broad peak at 578.5 nm is dominant, i.e. the formation of Eu_2O_3 is nearly avoided. Moreover, the optical

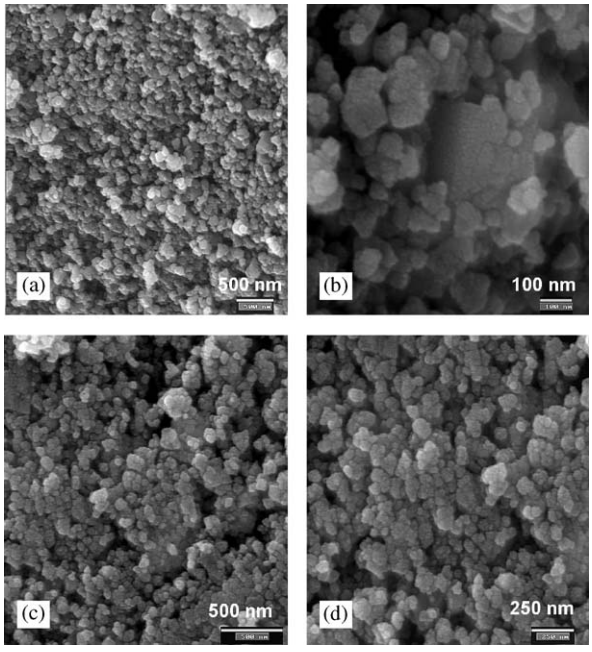

Fig. 2. SEM images showing the microstructure of GaN (a and b) and GaN:Eu 5% (c and d), obtained from nitrates, at different magnifications.

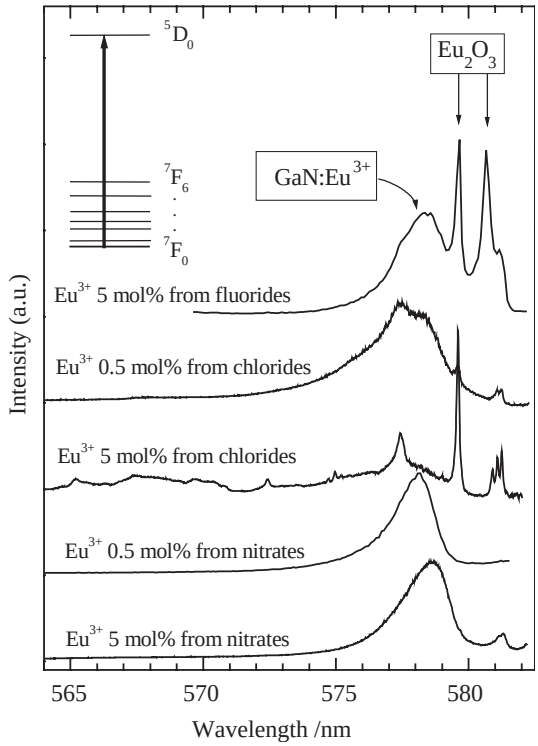

Fig. 3. Excitation spectra at 13 K of the $^5D_0$ level of the Eu^{3+} ions in GaN obtained from fluorides, chlorides or nitrates by detecting the $^5D_0 \rightarrow {}^7F_2$ transition at about 614 nm. The spectra have been normalized to the maximum intensity.

spectra of these samples did not appreciably change when they were left in air for at least 2 days.

A light red-shift of the 578.5 nm excitation peak is observed in the samples obtained from nitrates when the Eu^{3+} concentration is increased from 0.5 to 5 mol%. This effect was observed in other matrices and was explained considering energy transfer to lower energy Eu^{3+} ions in high concentrated samples [42].

The emission spectra from the $^5D_0$ to the ^7F_J levels have been measured for the different prepared materials. In Fig. 4, emission spectra of samples obtained from nitrates and from chlorides are shown together with the emission spectrum of microcrystalline Eu_2O_3. The spectrum of the sample obtained from nitrates shows lines inhomogeneously broaded due to the contribution of Eu^{3+} ions in a site distribution. Whereas, the spectra of the sample obtained from chlorides show the emission of Eu^{3+} ions in bcc and monoclinic Eu_2O_3 crystals [41], obtained after excitation at 577.5 and 579.5 nm, respectively. Fig. 4 also shows for comparison the room temperature spectrum of an Eu_2O_3 pellet, emission of Eu^{3+} ions in bcc and monoclinic Eu_2O_3 phases are observed due to simultaneous excitation of ions in these two crystalline phases.

FLN spectra have been measured in order to confirm that the broad excitation peak at 578.5 nm correspond to dispersed Eu^{3+} ions and not to any kind of

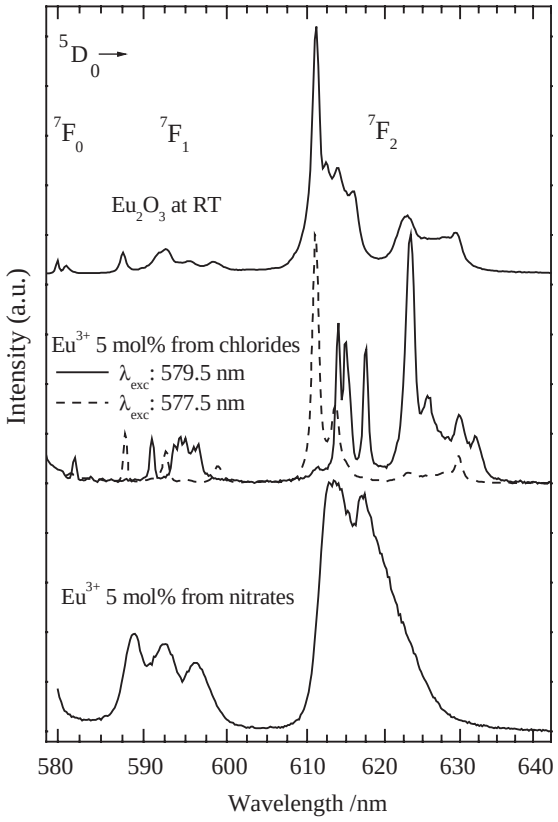

Fig. 4. Emission spectra from the $^5D_0$ level of the Eu^{3+} ions in GaN obtained from chlorides (laser excitation at 577.5 and 579.5 nm) or nitrates (broad band excitation at 578.5 nm) at 13 K and spectrum of Eu_2O_3 microcrystals (broad band excitation) at room temperature.

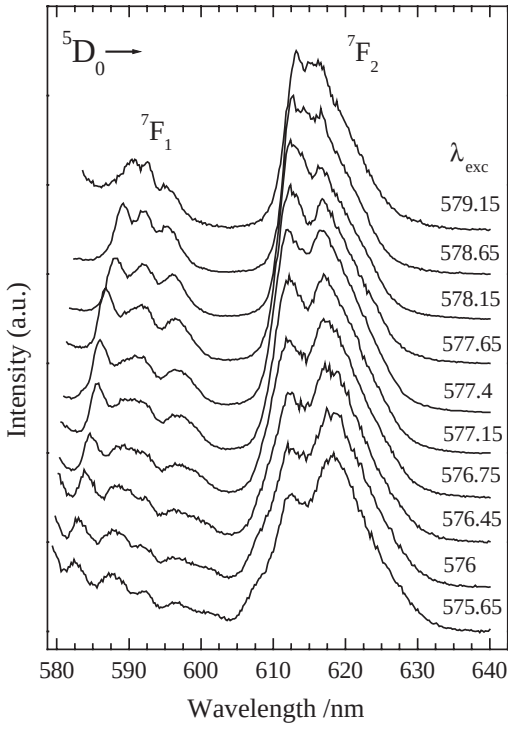

Fig. 5. FLN spectra at 13 K from the $^5D_0$ level of the Eu^{3+} ions in GaN obtained from nitrates by exciting at the wavelengths indicated in the figure.

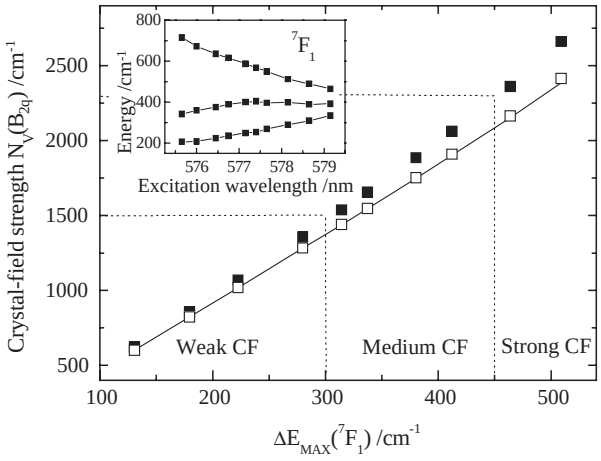

Fig. 6. Crystal-field strength parameter N_v (B_{2q}), with (■) and without (□) taking into account the J-mixing effect versus the maximum splitting of the $^7F_1$ multiplet in an Eu^{3+}-doped GaN. The solid line indicates the fit to the theoretical expression of Malta et al. [47]. Inset shows the energy of the $^7F_1$ Stark levels with respect to the $^7F_0$ ground level as a function of the excitation wavelength.

aggregated phase. After laser excitation at different wavelengths along the broad excitation peak at 578.5 nm, line narrowed emission spectra have been obtained in samples prepared from nitrates, as observed in Fig. 5. Moreover the emission spectra strongly depend on the excitation wavelength. The critical radius for the energy transfer between Eu^{3+} ions from the $^5D_0$ level is very short when compared with other rare earth ions, about 4.2 Å in oxides glasses [43]. The finding of FLN in our samples with low Eu^{3+} concentration (0.5 mol%) indicates that the energy transfer is not appreciable, i.e., the mean interionic distance is larger than the critical radius. These results indicate that the mean distance Eu^{3+}–Eu^{3+} is long enough to prevent energy transfer processes between them and, therefore, the Eu^{3+} ions are diluted and not in an aggregated phase.

The CF strength experienced by the Eu^{3+} ions in the GaN matrix is a measure of their electrostatic interaction with the surrounding ligands. The average strength of the crystal-field acting on the Eu^{3+} ions in GaN can be estimated from the splitting of the $^7F_1$ multiplets in to three Stark components. From the FLN measurements, positions of the $^7F_1$ Stark levels with respect to $^7F_0$ ground level are collected and plotted as a function of excitation wavelength in Fig. 6 (inset). The change in the energy positions of the $^7F_1$ Stark levels with excitation energy is attributed to the progressive increase in the magnitude of the local crystal-field acting on the Eu^{3+} ion. Higher crystal-field strength is due to larger charge

density and/or to a smaller Eu–ligand distance. As can be observed, the central $^7F_1$ Stark level deviates slightly with respect to the barycentre whereas low- and high-energy Stark levels vary largely with increase in excitation energy.

The splitting of the $^7F_1$ multiplet is only due to the second rank even crystal-field that, for orthorhombic and higher symmetries, is described in Wybourne's notation by the Hamiltonian [44],

$$H_{CF} = B_{20}C_0^{(2)} + B_{22}(C_{-2}^{(2)} + C_2^{(2)}), \quad (1)$$

where B_{20} and B_{22} are the crystal-field (CF) parameters.

The second rank CF parameters have been calculated by diagonalizing the Hamiltonian considering a C_{2v} local point symmetry for the Eu^{3+} ions, since it is the highest orthorhombic symmetry that allows full splitting of $^7F_1$ levels of the Eu^{3+} ion. Calculations include both those taking into account and those not taken into account the J-mixing effect between the ^7F_J multiplets. Moreover, some authors [45,46] have tried to simplify the description of the crystal-field defining a scalar, rotational invariant parameter called the CF strength. Using that given by Auzel and Malta [46], the second rank scalar CF strength parameter for orthorhombic symmetries takes the form

$$N_v(B_{2q}) = \sqrt{\frac{4\pi(B_{20}^2 + 2B_{22}^2)}{5}}. \quad (2)$$

This scalar magnitude can be related to the maximum splitting of the $^7F_1$ level as follows [43]

$$\Delta E_{MAX}(^7F_1) = \sqrt{\frac{0.3}{\pi(2+\alpha^2)}} N_v(B_{2q}), \quad (3)$$

where α is given by

$$\alpha = \frac{E_b - E_c}{\Delta E_{MAX}/2} \quad (4)$$

and E_b is the barycentre of energy of the $^7F_1$ level, calculated as the mean energy of the corresponding three Stark levels, whereas E_c is the energy of the central Stark level.

The scalar CF strength parameter calculated with the Eq. (2), considering only the second rank CF parameters 'with' and 'without J-mixing', as a function of maximum splitting of the $^7F_1$ level is shown in Fig. 6. A linear relation is observed when the influence of the nearby $^7F_2$ and $^7F_3$ multiplets, that mainly contribute to the J-mixing effect on the $^7F_1$ Stark levels, is not considered in the crystal-field calculation, and coincides with the theoretical relation, Eq. (3), obtained by Malta et al. [47]. The scalar CF strength calculated 'with J-mixing' shows a gradual deviation from the linear behavior for larger splittings showing, for a $^7F_1$ maximum splitting of about 510 cm^{-1}, an increase of more than 10% compared to that calculated 'without J-mixing'. This difference gives a measure of the influence of the J-mixing effect in the crystal-field analysis and is due to the gradual increase in the mixing of the wave functions of the $^7F_1$ Stark level, especially for the highest energy one with those of $^7F_2$ Stark levels.

Taking the J-mixing effect into account Görller-Walrand and Binnemans [44] have re-defined the 'weak crystal-field' (J-mixing negligible) and 'strong crystal-field' (J-mixing ineligible) for the lanthanide systems. According to this definition results given in Fig. 6 show that Eu^{3+} ions can be in this sample in a wide distribution of environments, going from 'weak' to 'strong crystal-field'. These results allow to make a rough distribution between weak ($\Delta E_{MAX}(^7F_1) < 300\,cm^{-1}$), medium ($300\,cm^{-1} < \Delta E_{MAX}(^7F_1) < 450\,cm^{-1}$) and strong ($\Delta E_{MAX}(^7F_1) > 450\,cm^{-1}$) CF environments [44]. Although it can be observed that in the GaN sample weak and medium crystal-field environments are mainly found, for those Eu^{3+} ions occupying strong crystal-field environments the J-mixing can be appreciable and it has to be taken into account in the calculations.

A comparison of the scalar CF strength values, calculated from CF parameters 'with J-mixing', as a function of excitation wavelength to $^5D_0$ level for different Eu^{3+} doped glasses [48–50] is shown in Fig. 7. It is found that the range of values obtained is similar to those found in glasses. This indicates that in the studied GaN samples there is a wide distribution of environments for the Eu^{3+} ions, comparable to the ones observed in glasses, with crystal-field strength values intermediate between the results for Be fluoride and Li fluoroborate glasses.

Finally, the excitation of the luminescent ions by interband excitation of the semiconductor and energy transfer to these ions is of practical importance for optoelectronic applications. In Fig. 8 emission spectra

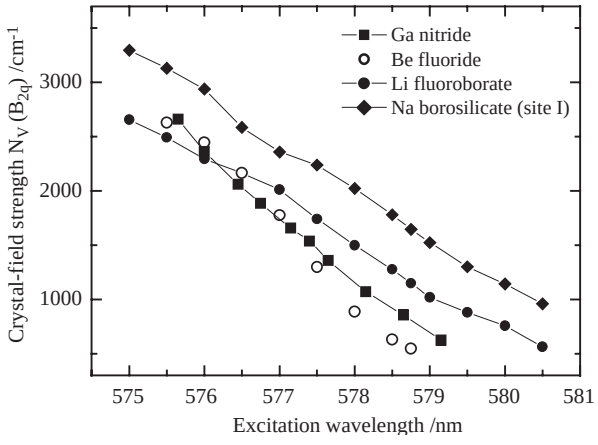

Fig. 7. Crystal-field strength parameter N_v (B_{2q}) as a function of the excitation wavelength to the $^5D_0$ level for GaN semiconductor (■) and fluoroberyllate (○) [49], lithium fluoroborate (●) [48] and sodium borosilicate (◆) [50] glasses.

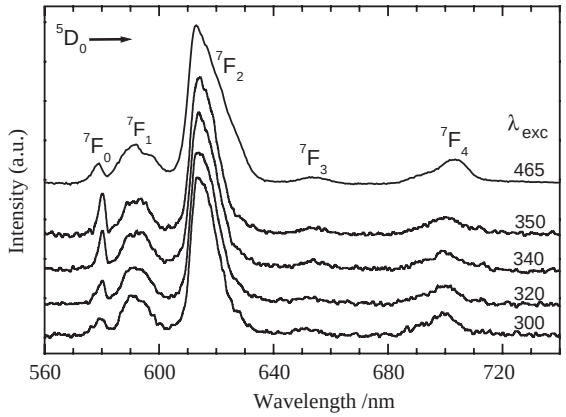

Fig. 8. Emission spectra from the $^5D_0$ level of the Eu^{3+} ions in GaN obtained from nitrates after direct excitation of the Eu^{3+} ions to the $^5D_2$ level (465 nm) or above-gap excitation (300, 320, 340 and 350 nm) at room temperature.

from the $^5D_0$ level of the Eu^{3+} ions in GaN prepared from nitrates after above-gap excitation (wavelength under 360 nm) are showed together with the emission spectrum obtained by direct excitation of these ions. The spectra obtained by above-gap excitation are very similar, with a light broadening of the Stark components (observed in the $^5D_0 \rightarrow {}^7F_0$ transition) when the excitation wavelength decreases meanwhile the splitting does not change appreciably (the overall bandwidth of the other transition does not change). A similar effect was observed in SnO:Eu^{3+} nanocrystals and was explained taking into account the dependence of the band gap with the nanocrystals radius, which takes to selectivity in the above-gap excitation [51]. On the other hand, the peaks in the spectra obtained by interband excitation are narrower than those obtained by direct excitation of the Eu^{3+} ions, as observed in Fig. 8. As a conclusion, the Eu^{3+} ions in strong crystal field environments are not excited efficiently by energy transfer from the semiconductor matrix.

When the emission spectra in Figs. 8 and 4 (samples obtained fro nitrates) are compared with results obtained in samples prepared by other methods, it is found that peaks are red-shifted and the Stark components are better resolved in samples prepared by MBE [52], MOCVD [53] and ion implantation [54]. Whereas, in samples obtained by sputtering [55] and by an ammonolysis process [35] the resolution of the Stark components and the position of the peaks appear to be more similar to the ones showed in this work.

4. Conclusions

Both single phase pure and Eu^{3+} doped GaN have been prepared in form of nanomaterials by ammonolysis of the corresponding freeze-dried precursor. It has been confirmed that freeze-dried precursor method is a simple and inexpensive technique to obtain rare-earth doped GaN, which can be an alternative to the relatively long processes of amides and azide precursors and to the use of expensive techniques as MOMBE. The optical spectra of the Eu^{3+} doped GaN show that the use of metallic nitrates as starting materials prevents the Eu_2O_3 formation, observed when metallic chlorides or fluorides were used. The excitation-wavelength dependence in the FLN spectra is indicative of large distances Eu^{3+}–Eu^{3+} confirming that the Eu^{3+} ions are uniformly spreaded. The Eu^{3+} ions occupy a wide distribution of environments, characterized by a wide range of crystal-field values, comparable to the ones found in glasses.

Acknowledgments

This research has been supported by Spanish research programs MCYT (MAT 2001-3334 and MAT 2001-3363), 'Gobierno de Canarias' (PI2001/053 and PI 2001/048) and Universidad de La Laguna (ULL 2004). A.E.-H. wishes to thank "Agencia Española de Cooperación Internacional" for financial support and D.P.C. to "Ministerio de Educación, Cultura y Deportes" for a grant (F.P.U.)

References

[1] H. Morkoç, S.N. Mohammad, Science 51 (1995) 267.
[2] T. Matsuoka, Adv. Mater. 8 (6) (1996) 496.
[3] M.J. Taylor, P.J. Brothers, in: A.J. Downs (Ed.), The Chemistry of Aluminium, Gallium, Indium and Thallium, Blackie-Chapman Hall, New York, 1993.
[4] (a) G.P. Pomrenke, P.B. Klein, D.W. Lange (Eds.), Rare earth Doped Semiconductors, Mater. Res. Soc. Symp. Proc., vol. 301, MRS, Pittsburgh, PA, 1993;
(b) S. Cotta, A. Polman, R.N. Schwartz (Eds.), Rare Earth Doped Semiconductors II, Mater. Res. Soc. Symp. Proc., vol. 422, MRS, Pittsburgh, PA, 1996.
[5] M. Thaik, U. Hommerich, R.N. Schwartz, R.G. Wilson, J.M. Zavada, Appl. Phys. Lett. 71 (1997) 264.
[6] W. Chen, G. Li, J.O. Malm, Y. Huang, R. Wallenberg, H. Han, Z. Wang, J.O. Bovin, J. Lumin. 91 (2000) 139, and reference there in.
[7] T. Detchprohm, K. Hiramatsu, I. Sawaki, I. Akasaki, J. Cryst. Growth 137 (1994) 171.
[8] L. Baixia, L. Yinkui, J. Mater. Chem. 3 (1993) 117.
[9] D.C. Boyd, R.T. Hash, D.R. Mantel, R.K. Schulze, J.F. Evans, W.L. Ladfelter, Chem. Mater. 1 (1989) 119.
[10] M.A. Khan, J.N. Kuznia, J.M. Van Hove, D.T. Olson, Appl. Phys. Lett. 58 (1991) 526.
[11] A. Miehr, M.R. Mattner, R.A. Fischer, Organometallics 15 (1996) 2053.
[12] S.J. Nakamura, J. Cryst. Growth 179 (1997) 11.
[13] S. Nakamura, T. Mukai, M. Senoh, S. Nagahama. N. J. Iwasa, Appl. Phys. 74 (1993) 3911.
[14] R. Niebuhr, K. Bachem, K. Dombrowski, M. Maier, W. Pletschen, U.J. Kaufmann, Electron. Mater. 24 (1995) 1531.

[15] J. McMurran, D. Dai, K. Balasubramanian, C. Steffek, J. Kouvetakis, J. Hubbard, Inorg. Chem. 37 (1998) 6638.
[16] J. Kouvetakis, J. McMurran, P. Mastunaga, M. O'Keefe, J.L. Hubbard, J. Inorg. Chem. 36 (1997) 1792.
[17] V. Lakhotia, D.A. Neumayer, A.H. Cowley, R.A. Jones, J.G. Ekerdt, Chem. Mater. 7 (1995) 546.
[18] (a) A. Devi, H. Sussek, H. Pritzkow, M. Winter, R.A. Fischer, Eur. J. Inorg. Chem. 12 (1999) 2127;
(b) O. Contreras, S. Srinivasan, F.A. Ponce, G.A. Hirata, F. Ramos, J. McKittrick, Appl. Phys. Lett. 81 (2002) 1993.
[19] A. Devi, W. Rogge, A. Wohlfart, F. Hipler, H. Becker, H. Sussek, R.A. Fischer, Chem. Vap. Deposit. 6 (2000) 245.
[20] A. Frank, F. Stowasser, H. Sussek, H. Pritzkow, C.R. Miskys, O. Ambacher, M. Giersig, R. Fischer, J. Am. Chem. Soc. 120 (1998) 3512.
[21] A. Manz, A. Birkner, M. Kolbe, R. Fischer, Adv. Mater. 12 (2000) 569.
[22] D.M. Hoffman, S.P. Rangarajan, S.D. Athavale, D.J. Economou, J.-R. Liu, Z. Zheng, W.-K. Chu, J. Vac. Sci. Technol. A 14 (2) (1996) 306.
[23] H.S. Park, S.D. Waezsada, A.H. Cowley, H.W. Roesky, Chem. Mater. 10 (1998) 2251.
[24] J.F. Janik, R.L. Wells, Chem. Mater. 8 (1996) 2708.
[25] J.F. Janik, R.L. Wells, J.L. Coffer, J.V. John, W.T. Pennington, G.L. Schimek, Chem. Mater. 10 (1998) 1613.
[26] O.I. Micic, S.P. Ahrenkiel, D. Bertram, A.J. Nozik, J. Appl. Phys. Lett. 75 (1999) 478.
[27] J.W. Hwang, J.P. Campbell, J. Kozubowski, S.A. Hanson, J.F. Evans, W.L. Gladfeter, Chem. Mater. 7 (1995) 517.
[28] J. Jegier, S. McKernan, A.P. Purdy, W.L. Gladfelter, Chem. Mater. 12 (2000) 1003.
[29] G. Chaplais, S. Kaskel, J. Mater. Chem. 14 (2004) 1017–1025.
[30] L. Grocholl, S.A. Cullison, J. Wang, D.C. Swenson, E.G. Gillan, Inorg. Chem. 42 (2002) 2920.
[31] C.M. Balkas, R.F. Davis, J. Am. Ceram. Soc. 79 (1996) 2309.
[32] G.L. Wood, E.A. Pruss, R.T. Paine, Chem. Mater. 13 (2001) 12.
[33] R. García, G.A. Hirata, M.H. Farías, J. McKittrick, Mater. Sci. Eng. B 90 (2002) 7.
[34] J.M. Zavada, M. Thaik, U. Hommerich, J.D. MacKenzie, C.R. Abernathy, S.J. Pearton, R.G. Wilson, J. Alloy. Compd. 300 (2000) 207.
[35] G.A. Hirata, F. Ramos, R. García, E.J. Bosze, J. Mckittrick, O. Contreras, F.A. Ponce, Phys. Stat. Sol. (a) 188 (2001) 179–182.
[36] J. Heikenfeld, M. Garter, D.S. Lee, R. Birkhahn, A.J. Steckl, Appl. Phys. Lett. 75 (1989) 1189.
[37] S. Morishima, T. Maruyam, K. Akimoto, J. Cryst. Growth 209 (2000) 378.
[38] T. Roisnel, J. Rodríguez-Carvajal, WinPLOTR: a windows tool for powder diffraction patterns analysis, in: R. Delhez, E.J. Mittenmeijer (Eds.), Materials Science Forum, Proceedings of the Seventh European Powder Diffraction Conference (EPDIC 7), 2000, p. 118–123.
[39] (a) S. Strite, H. Morkoc, J. Vac. Sci. Technol. B 10 (1992) 1237;
(b) D.A. Neumayer, J.G. Ekerdt, Chem. Mater. 8 (1996) 9.
[40] A.R. West, Solid State Chemistry and its Applications, Wiley, Chichester, 1984, pp. 173–175.
[41] K.C. Sheng, G.M. Korenowski, J. Phys. Chem. 92 (1988) 50.
[42] V. Lavín, I.R. Martín, U.R. Rodríguez-Mendoza, V.D. Rodríguez, J. Phys.: Condens. Matter 11 (1999) 8739.
[43] J. Méndez-Ramos, V. Lavín, I.R. Martín, U.R. Rodríguez-Mendoza, V.D. Rodríguez, A.D. Lozano-Gorrín, J. Appl. Phys. 89 (2001) 5307.
[44] G. Görller-Walrand, K. Binnemans, Handbook of the Physics and Chemistry of Rare Earths, vol. 23, 1996, p. 121.
[45] R.P. Leavitt, J. Chem. Phys. 77 (1982) 1661.
[46] F. Auzel, O.L. Malta, J. Phys. (France) 44 (1983) 201.
[47] O.L. Malta, E. Antic-Fidancev, M. Lemaitre-Blaise, A. Milicic-Tang, M. Taibi, J. Alloys Compd. 228 (1995) 41.
[48] V. Lavín, P. Babu, C.K. Jayasankar, I.R. Martín, V.D. Rodríguez, J. Chem. Phys. 115 (2001) 10935.
[49] C. Brecher, L.A. Riseberg, Phys. Rev. B 21 (1980) 2607.
[50] G. Pucker, K. Gatterer, H.P. Fritzer, M. Betinelli, M. Ferrari, Phys. Rev. B 53 (1996) 6225.
[51] A.C. Yanes, V.D. Rodríguez, J. del-Castillo, M.E. Torres, J. Peraza, Appl. Phys. Lett., in press.
[52] U. Hömmerich, E.E. Nyein, D.S. Lee, J. Heikenfeld, A.J. Steckl, J.M. Zavada, Mater. Sci. Eng. B 105 (2003) 91.
[53] M. Pan, A.J. Steckl, Appl. Phys. Lett 83 (2003) 9.
[54] T. Monteiro, C. Boemare, M.J. Soares, R.A. Sá Ferreira, L.D. Carlos, K. Lorenz, R. Vianden, E. Alves, Physica B 308 (2001) 22.
[55] J.H. Kim, P.H. Holloway, J. Appl. Phys. 95 (2004) 4787.